Electronic Supplementary Material (ESI) for Physical Chemistry Chemical Physics.

Supporting Information

Revealing the Impact of Thermal Annealing on Perovskite/Organic Bulk Heterojunction Interface in Photovoltaic Device

Peng Chen[a], Xinyuan Ma[a], Zhiyu Wang[a], Nan Yang[a], Jianwen Luo[a], Ke Chen[a*], Pengyi Liu[a], Weiguang Xie[a], and Qin Hu[b*]

[a] Siyuan Laboratory, Guangdong Provincial Engineering Technology Research Center of Vacuum Coating Technologies and New Energy Materials, Department of Physics, Jinan University, Guangzhou, Guangdong 510632, China

[b] School of Microelectronics, University of Science and Technology of China, Hefei, Anhui 230026, China

Corresponding E-mail addresses:

chenke@email.jnu.edu.cn (Ke Chen),

qinhu20@ustc.edu.cn (Qin Hu)

1. Supplementary Figures

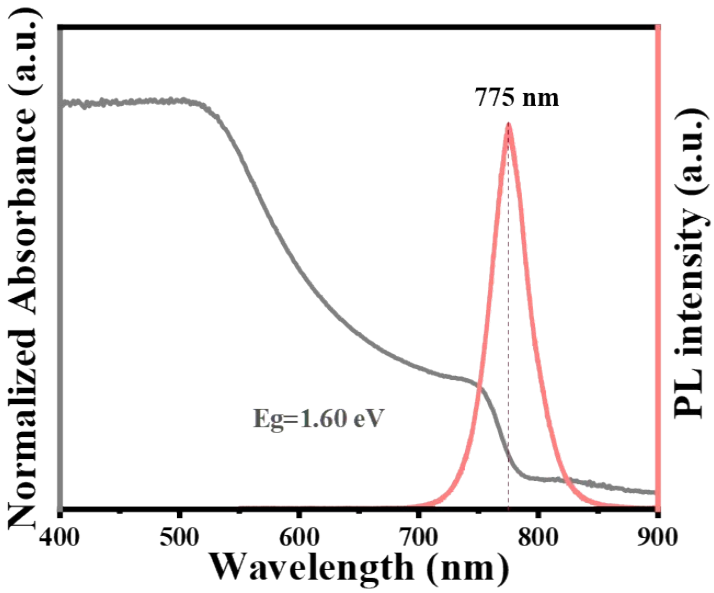

Figure S1. Photoluminescence (PL) and ultraviolet-visible (UV-Vis) absorption spectra of perovskite thin films.

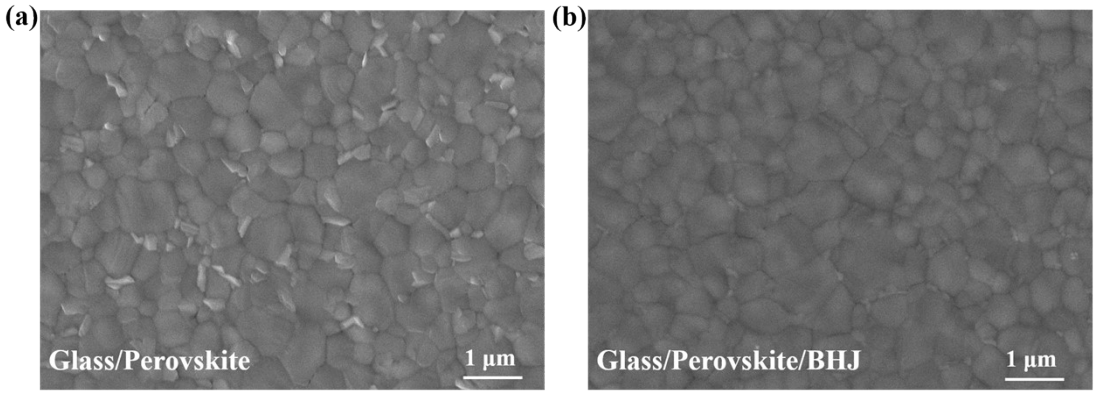

Figure S2. SEM images of the perovskite film and perovskite/BHJ film.

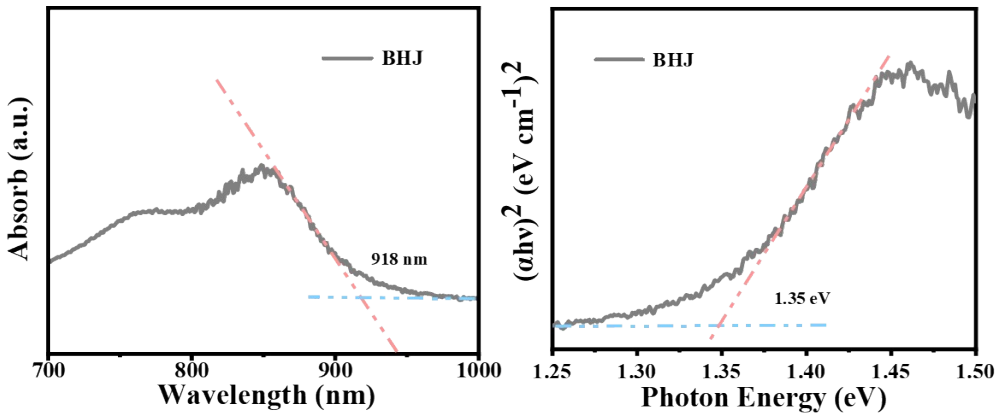

Figure S3. Ultraviolet-visible (UV-Vis) absorption spectra and Tauc plot results to determine the bandgap of BHJ.

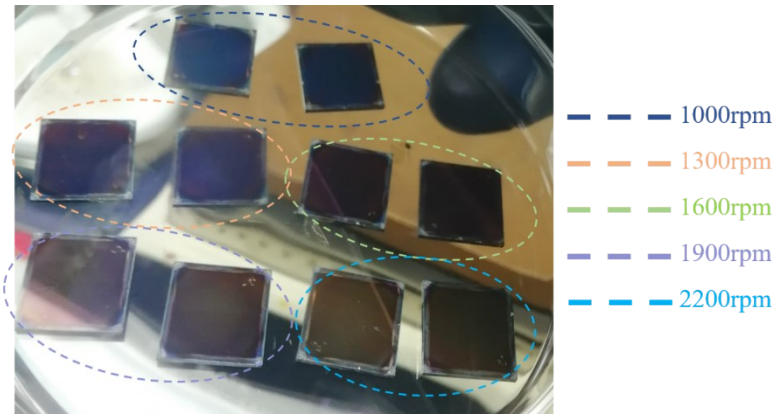

Figure S4. Photographs of the BHJ films under different spin-coating speed to allow readers to visually see the effects of different spinning speeds on film formation. In fact, this is to determine the spinning speed corresponding to the BHJ thin film with optimal performance. As the rotational speed decreases, the film surface color gradually changed from bright gold to dark gold.

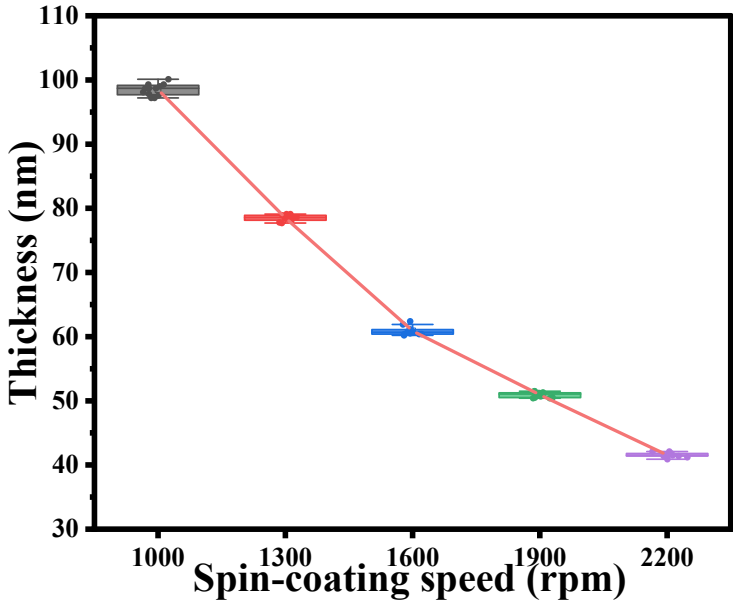

Figure S5. BHJ film thickness under different spin-coating speed. We measured the thickness of both the center and edge area of the film, and then calculated the average film thickness value.

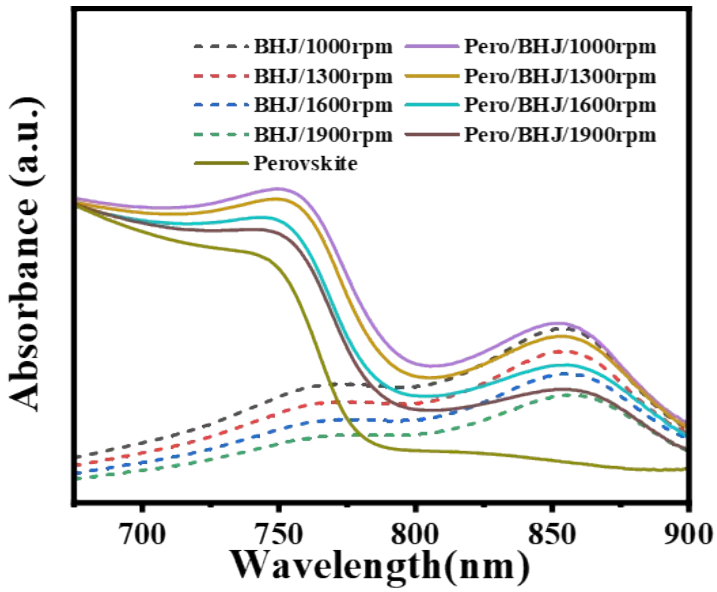

Figure S6. UV–vis absorption spectra of perovskite, BHJ and integrated perovskite/BHJ films with varied film thickness by controlling the solution spin-coating speed. The measurements were conducted in ambient environment with temperature of 25°C and relative humidity of 50%. The sampling area is 1mm ×10mm near the film center.

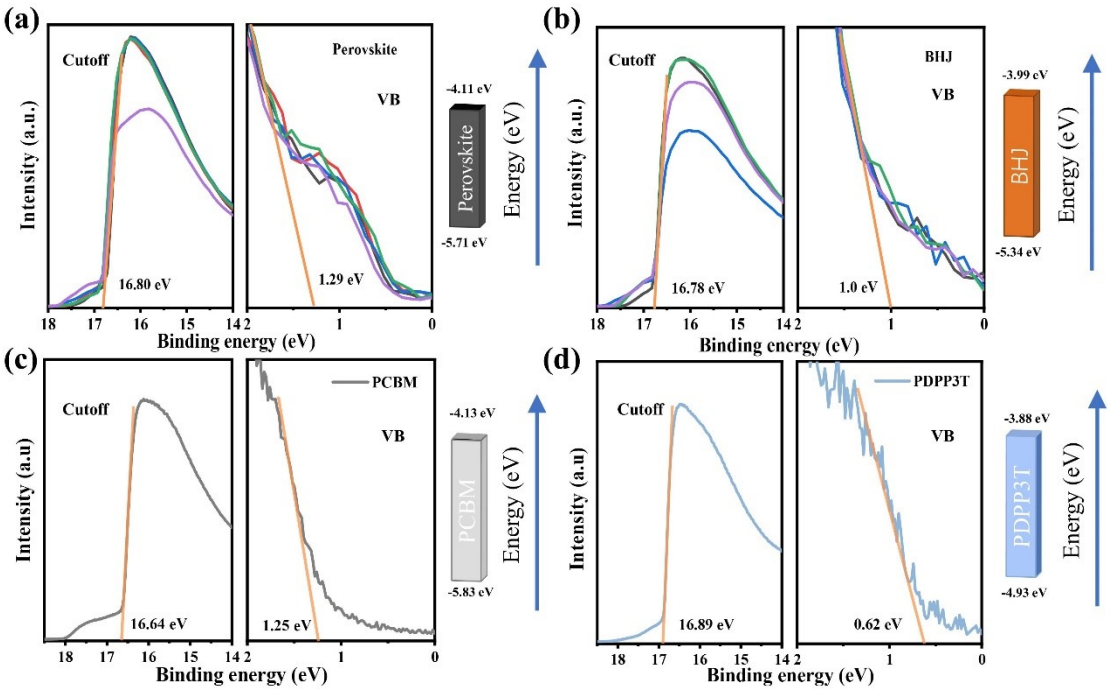

Figure S7. UPS spectra of (a) perovskite, (b) BHJ, (c) $PC_{61}BM$ and (d) PDPP3T thin film and the schematic illustration of their energy levels. The Fermi binding energy of the apparatus is 0 eV. The exact band level values were determined using the following formulas:

$$W_F = h\nu - E_{Cutoff} \quad (1)$$

$$E_{Fermi} = E_{vacuum} - W_F \quad (2)$$

$$VBM = -h\nu + E_{Cutoff} - E_{VB} \quad (3)$$

$$CBM = VBM + E_g \quad (4)$$

Among them, $h\nu$ is the energy of the incident photon. The binding energy of helium ultraviolet ray that we used to test is 21.22 eV. E_{cutoff} is the value corresponding to the cutoff edge of the secondary electron, which is the value of the material's escape work. E_{Fermi} is the Fermi level, E_{vaccum} is the vacuum level (0 eV), VBM is the valence band maximum, E_{VB} is the energy offset between Fermi level and valence band maximum, CBM is the conduction band minimum, and Eg is the material's bandgap value. For perovskite, E_{VB} is 1.29 eV, with E_{Cutoff} = 16.80 eV, VBM = -5.71 eV. The absorption edge of the perovskite film is approximately 775 nm, corresponding to a

bandgap value of 1.60 eV. Therefore, the CBM can be estimated as -4.11 eV[1,2,3]. Other calculations follow the same method.

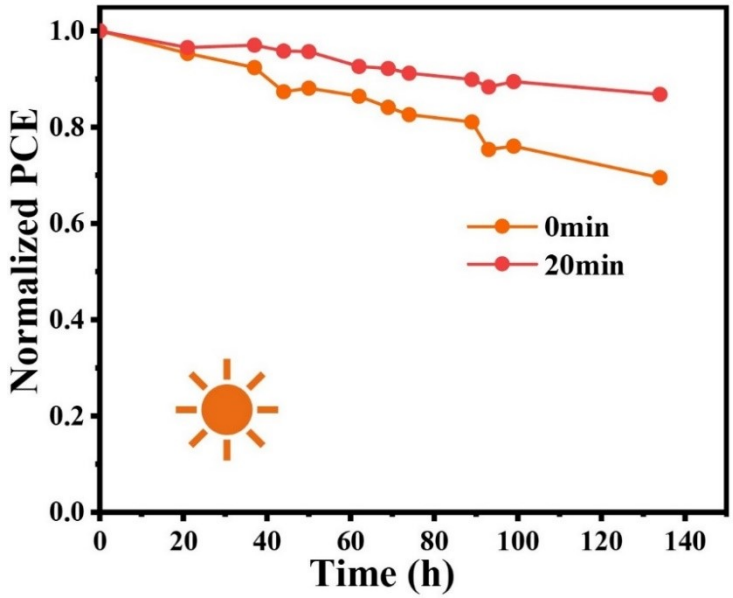

Figure S8. Operation stability testing of the unpacked devices under continuous illumination using a white LED lamp (100mW/cm^2) at room temperature in a glove box filled with N_2. After 140 hours, the device annealed for 20 minutes maintained 86.8% of its original efficiency, while the unannealed devices decreased to 65.9% of its initial efficiency.

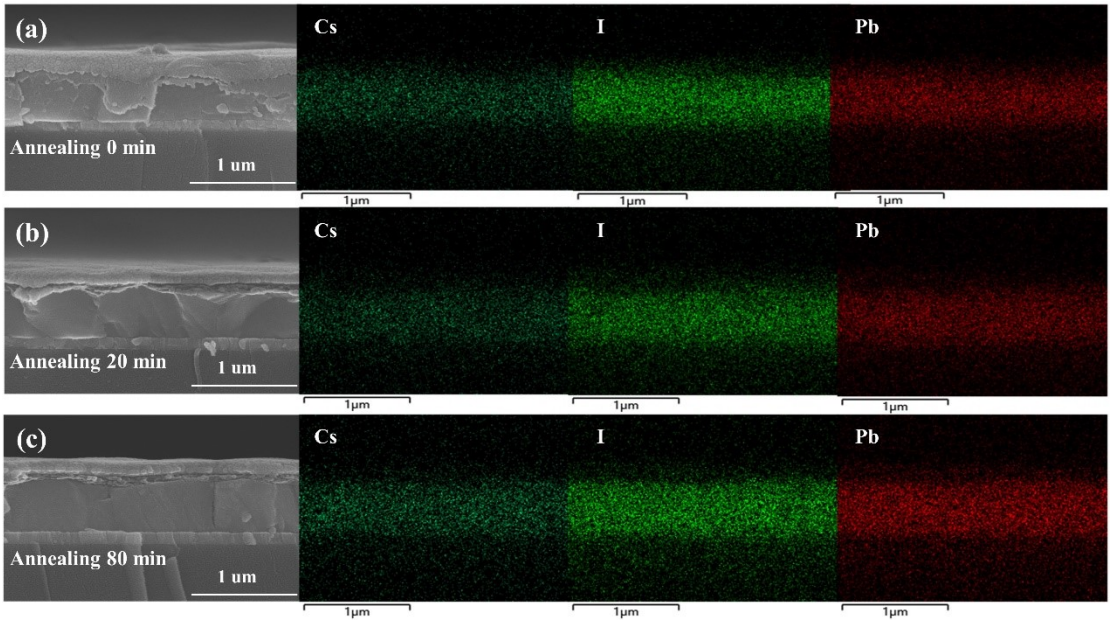

Figure S9. SEM-EDX analysis of material elements distribution at the perovskite/BHJ interface with varied thermal annealing treatment durations: (a) 0 minute, (b) 20 minutes, and (c) 80 minutes.

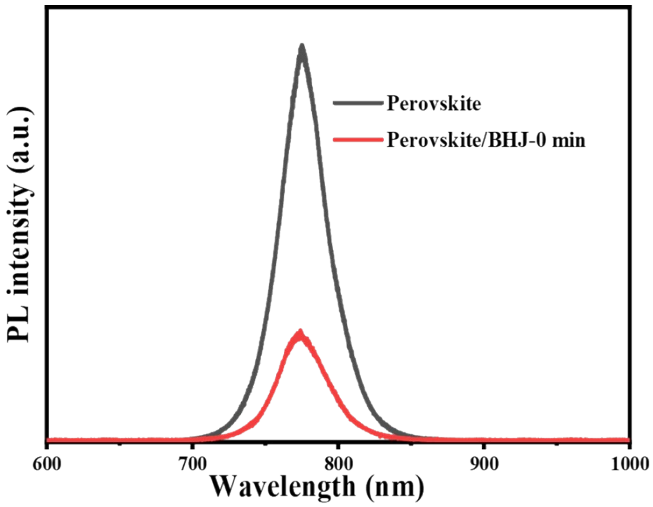

Figure 10. PL spectra images of perovskite thin film and integrated perovskite/BHJ film annealed for 0 minute.

2. Supplementary Tables

Table S1. BHJ film mean-thickness under different spin-coating speed.

Spin-coating Speed	Film thickness (nm)
1000rpm/30s	98.5
1300rpm/30s	78.5
1600rpm/30s	60.1
1900rpm/30s	50.9
2200rpm/30s	41.5

Table S2. Detailed photovoltaic performance parameters of the integrated perovskite/BHJ devices corresponding to different annealing times.

annealing time(min)	**V_{oc} (V)**	**J_{sc} (mA/cm^2)**	**FF (%)**	**PCE (%)**
0	1.071	23.924	78.8	20.244
10	1.071	24.64	79.7	21.027
20	1.053	24.763	82.7	21.578
40	1.048	24.759	82.3	21.357
50	1.061	24.456	81.6	21.163
60	1.056	23.97	82.1	20.787
80	1.039	24.026	81.4	20.312

3. Supplementary Notes

Supplementary Notes 1. Principle of TAS

In principle, transient absorption spectroscopy is a technique that detects signals as they change over time. In the process, there is initially a laser beam used to excite the sample, referred to as the pump light source. Then, another beam of light is used to measure the sample's absorbance as a function of time, known as the probe light source. Using this technique to measure charge transfer between perovskite and BHJ layers essentially involves observing changes in the electronic states within the material during an extremely short interval after the excitation of the perovskite layer by the light source. In transient absorption spectroscopy, we do not directly measure absorbance but instead measure transmittance. For this purpose, we make the following definition:

$$A = -\log T = \log \frac{P_0}{P}$$

In the equation, A represents absorbance, which is the negative logarithm of transmittance (T), and P_0 and P are the intensities of light measured before and after passing through the sample, respectively. At time zero:

$$A(0) = \log \frac{P_0(0)}{P(0)}$$

$P_0(0)$ represents the incident light intensity, and $P(0)$ represents the light intensity after passing through the sample. After a time t, the incident light intensity remains constant while the light intensity passing through the sample changes, following:

$$A(t) = \log \frac{P_0(0)}{P(t)}$$

Taking the difference between the two equations, we get:

$$A(t) - A(0) = \Delta A = \log \frac{P(0)}{P(t)}$$

This corresponds exactly to the differential spectra observed in the main manuscript Fig. 5a-b.

As mentioned earlier, after molecules are excited from the ground state to the excited state by the pumping light, the probe light source can induce radiation, causing

stimulated emission in the perovskite layer, manifested as negative peaks in the differential spectrum at 680-700nm. Because the probe light appears to have more light transmission when projected onto the sample as a second light source, it actually results from the photons emitted reaching the detector, hence appearing as negative peaks.

The process of electrons in the perovskite layer transitioning from the excited state to another excited state is non-existent relative to ground state matter. However, when the pumping light excites electrons in the perovskite layer to the excited state, such transitions from the excited state to another excited state occur, leading to observation of positive peaks in the differential spectrum at 740-760nm, known as the excited state absorption (ESA) peak. It can be observed that for the film after annealing for 20 minutes, the peaks in the differential spectrum are more uniform, indicating fewer cases of carrier recombination during excitation.

Reference

1 A. Agresti, A. Pazniak, S. Pescetelli, A. Di Vito, D. Rossi, A. Pecchia, M. Auf Der Maur, A. Liedl, R. Larciprete, D. V. Kuznetsov, D. Saranin and A. Di Carlo, Titanium-carbide MXenes for work function and interface engineering in perovskite solar cells, *Nat. Mater.*, 2019, **18**, 1228–1234.

2 K. Yan, J. Chen, H. Ju, F. Ding, H. Chen and C.-Z. Li, Achieving high-performance thick-film perovskite solar cells with electron transporting Bingel fullerenes, *J. Mater. Chem. A*, 2018, **6**, 15495–15503.

3 X. Zhou, L. Zhang, J. Yu, D. Wang, C. Liu, S. Chen, Y. Li, Y. Li, M. Zhang, Y. Peng, Y. Tian, J. Huang, X. Wang, X. Guo and B. Xu, Integrated Ideal-Bandgap Perovskite/Bulk-Heterojunction Solar Cells with Efficiencies > 24%, *Adv. Mater.*, 2022, **34**, 2205809.